Missile Impact on SC Walls: Global Response

William H. Johnson, F ASCE[1], Jakob Bruhl, M ASCE[2], Damon G. Reigles, M ASCE[3], Jie Li, M ASCE[4], Amit H. Varma, M ASCE [5]

[1]Principal Engineer, Bechtel Power Corporation, 5275 Westview Drive, Frederick, MD 21703; PH (301) 228-7747; email: whjohnso@bechtel.com
[2]PhD Candidate, School of Civil Engineering, Purdue University, West Lafayette, IN 47907; email: jbruhl@purdue.edu
[3]Senior Engineer, Bechtel Power Corporation, 5275 Westview Drive, Frederick, MD 21703; PH (301) 228-7725; email: dgreigle@bechtel.com
[4]Senior Engineer, Bechtel Power Corporation, 5275 Westview Drive, Frederick, MD 21703; jli@bechtel.com
[5]Associate Professor, School of Civil Engineering, Purdue University, West Lafayette, IN 47907; PH (765) 496-3419; email: ahvarma@purdue.edu

ABSTRACT

Steel plated composite concrete (SC) walls, which consist of a poured concrete core between two studded steel plates, have been utilized in many applications in lieu of conventional reinforced concrete (RC) walls. For this type of wall, the steel reinforcing plates serve as formwork, which allows for modularization of the design and correspondingly accelerated construction. Recently, both overseas and domestic nuclear power plant (NPP) projects have incorporated SC walls into their designs. When installed in nuclear plant facilities, such walls may be required to resist the effects of extreme loadings such as tornado missile and aircraft impact. The analysis of the structural response of conventional RC walls to such extreme loadings is well understood and is amenable to a simplified and well known inelastic single-degree-of-freedom (SDOF) approach which treats the wall as an effective mass with an easily defined inelastic spring. The purpose of this investigation is to study the SC wall load deformation behavior or resistance function, under missile impact, for input to an SDOF model. Based on pseudo-static nonlinear finite element analyses, the SC wall load deformation behavior under a central concentrated load is investigated for some typical wall panel configurations. System parameters are varied to assess their effects on the resistance function.

INTRODUCTION

The simplified single-degree-of-freedom (SDOF) evaluation methodology for the global inelastic response of conventional reinforced concrete (RC) panel structures for their response to impact loads is well known and is described in Biggs (1964), ASCE Manual of Practice No. 58 (1980) and UFC 3-340-02 (2008). Such response, which is characterized by the development of a collapse mechanism and by deformation of the plate through rotation of the plastic hinges is distinctly different from the localized perforation, penetration, or scabbing response. For RC plate

structures, equations to estimate this local response have long been available, and more recently, local relations for the impact resistance of steel-plated composite concrete (SC) walls and slabs have been developed (Tsubota et al., 1993; Mizuno et al., 2005; Bruhl et al., 2013). To date, no global response calculation methodology based on the demonstrated global impact behavior of SC wall structures is available. Such a demonstration is complicated by SC wall construction with its variety of components: shear studs, steel plates, tie bars, and plain concrete. This investigation studies the behavior of SC structures, using nonlinear finite element solutions, for the purpose of developing an SDOF response solution approach analogous to that for RC walls. In addition to the absence of a verified method for determination of the SC wall impact structural response, there are also no criteria for the acceptance of such response, such as limiting response ductility, plastic hinge rotations, limiting values for stud and tie bar spacing and dimensions, etc. Based on the behavior and limiting conditions determined from these solutions, acceptance criteria are developed.

METHODOLOGY

The global geometric similarity of SC and RC panels naturally suggests extension of the SDOF approach for RC structures to SC structures. Consider a generalized SDOF equation of equilibrium for such an RC or SC system

$$M_e[x(t)]\ddot{x}(t) + R[x(t)]x(t) = F(t) \qquad (1)$$

where $M_e[x(t)]$ is a response level dependent effective mass, $R[x(t)]$ is a response level dependent resistance and $F(t)$ is an applied impulse. For conventional RC walls, the resistance function is elastic, perfectly plastic. Studies from a number of FE runs (cases studied are summarized in Table 1) indicate considerable strain hardening after steel plate first yielding for SC walls, so that $R[x(t)]$ for SC walls is more appropriately represented as bilinear strain hardening (Figure 1).

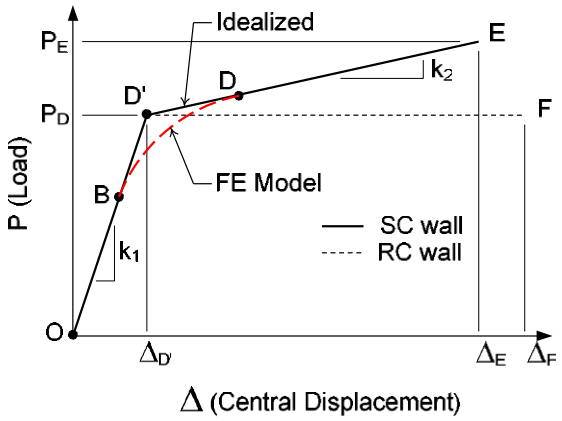

Figure 1. Resistance Functions for RC and SC Walls.

Since the SDOF inelastic method for plate structures assumes a response with a shape function defined by the collapse mechanism, which is dependent only on the plate global geometry, global mass considerations are essentially the same for RC and

SC plates. Thus $M_e[x(t)]$ for an SC plate is calculated in accordance with the mass factor K_m, for RC plates, based on the response level (Biggs, 1964; ASCE Manual of Practice No. 58, 1980; and UFC 3-340-02, 2008). In the equilibrium equation, then, $M_e[x(t)]$ is as a constant, same as for RC walls and $R[x(t)]$ is taken as a bilinear function of x. While this prohibits use of the response chart for determination of the response ductility, the response is easily determined iteratively from the finite difference recursion relation.

$$x(t_{i+1}) = \frac{F(t_i) - \{k_1(H[x_0 - x(t_i)])x(t_i) + (1 - H[x_0 - x(t_i)])(R_0 + k_2[x(t_i) - x_0])\}}{M_e[x(t_i)]}(\Delta t)^2 + 2x(t_i) - x(t_{i-1}) \quad (2)$$

where k_1 is the elastic stiffness, k_2 is the stiffness of the "strain-hardening" portion of the bilinear load-displacement function and R_0 is the resistance at yield.

The sections which follow study the resistance function, R, for SC panels and the effect of system parameters on its behavior. These studies are performed using fixed edge and simply supported FE models subject to small footprint pseudo-static loads.

FINITE ELEMENT MODEL FOR DEVELOPMENT OF THE RESISTANCE FUNCTION

This section focuses on two things: (1) demonstration, by example, of how to build an SC panel FE model for generation of the resistance function, and (2) investigation of the ranges of system parameters to assure desired ductile behavior. This demonstrative rather than prescriptive approach for definition of the resistance function is necessary as SC panel behavior is not yet sufficiently understood to develop a prescription. Future investigations will develop prescriptive guidelines which eliminate the need for such analyses, but for now, each wall panel impact analysis effort must develop its own resistance function by way of FE analysis. The intent of the model is to capture, in correct sequence, the progressive failure behavior of the SC panel system elements. A pseudo-static analysis is selected, as once the plate has yielded, the deflected shape defined by the collapse mechanism varies little. This behavior is analogous to that for an RC panel. LS-DYNA (LSTC, 2012) is used for the finite element analysis.

Typical exterior and interior NPP walls are either rectangular flat plate structures or sectors of cylindrical shells. Figure 2 shows a typical SC wall section comprised of concrete, steel plates, tie-bars and shear studs. The strength requirements for proportioning of these various system elements are provided in the forthcoming Appendix N9 of AISC N690 (Draft). The FE model studies for investigation of resistance function behavior, therefore, will consider only parameter ranges which satisfy the N690 requirements.

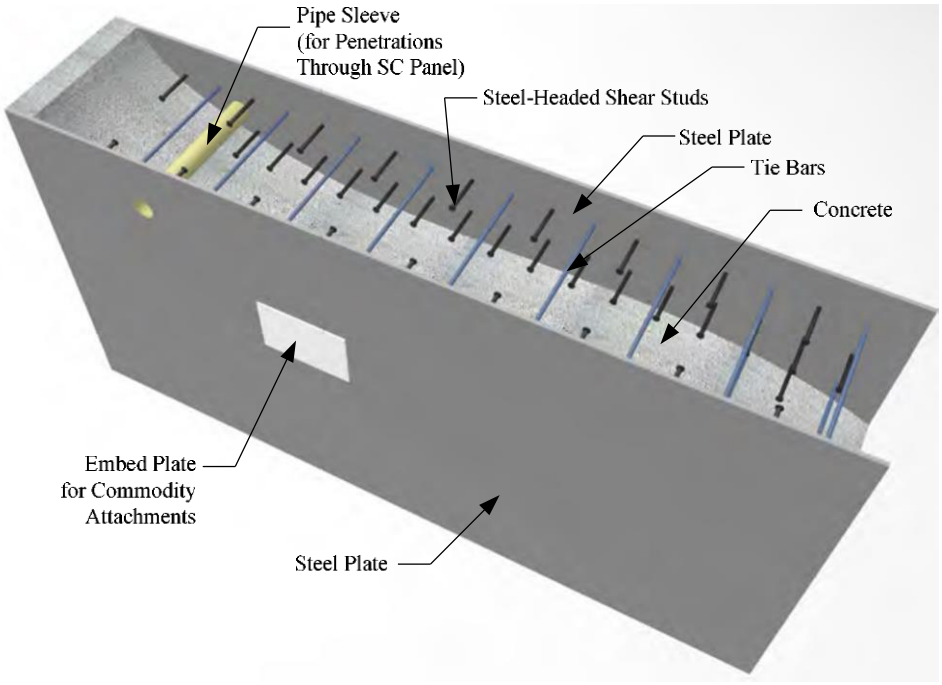

Figure 2. Typical SC Wall Section.

Figures 3 and 4 depict the model, which consists of 11 layers of concrete solid brick elements, an upper and lower steel plate connected with tie bars, shear studs attaching the plates to the concrete, and a rigid plate to apply the load to the panel. Solid elements were used for the concrete and steel plates. Beam elements were used for the tie bars and shear studs. Concrete was modeled with LS-DYNA material MAT_159 (Murray, 2007; LSTC, 2012) and steel was modeled using LS-DYNA Piecewise Linear Plasticity material MAT_024 (LSTC, 2012). The idealized stress-strain curve for the Grade 50 steel plate and tie bars was developed from an extensive database of tension coupon tests (Varma, 2000). Other material parameters are set as follows: effective uniaxial failure strain at 0.146 for steel plate and 0.05 for tie bars and shear studs, f_c' = 5000 psi, and pre-existing damage variable to account for shrinkage at 0.65. Tie bars and studs were mathematically embedded in the concrete using a penalty coupling mechanism (LS-DYNA keyword CONSTRAINED_ LAGRANGE_ IN_SOLID) which assumes perfect bond with the concrete.

To account for load-slip behavior of shear studs, the beam element studs were connected to the steel plate using connector elements as explained by Zhang et al. (2013). The zero-length connector element consists of a single discrete beam element. Its material (LS-DYNA material MAT_068 [LSTC, 2012], Nonlinear Plastic Discrete Beam) is defined with the load-slip relationship shown experimentally and explained by Shim et al. (2004) and Anderson and Meinheit (2000). The expected maximum slip was calculated and used as the failure criteria in the connector element material definition. Connector elements share nodes with the beam modeling the stud and the steel plate. This modeling method provides realistic stud, concrete, and steel plate interaction as it accounts for the stud embedded in concrete, welded to the steel plate, deformation of the stud, and stud shank failure. Rigid circular plate nodes are allowed to separate from the top steel plate upper nodes during application of the load.

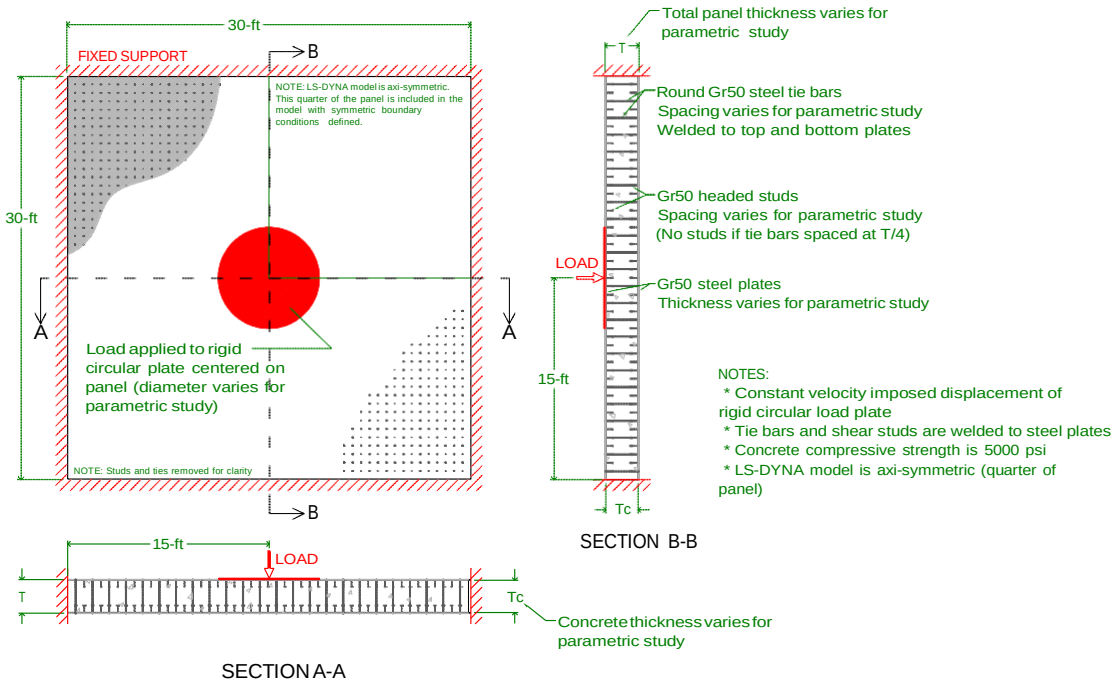

Figure 3. Typical SC Wall FE Model.

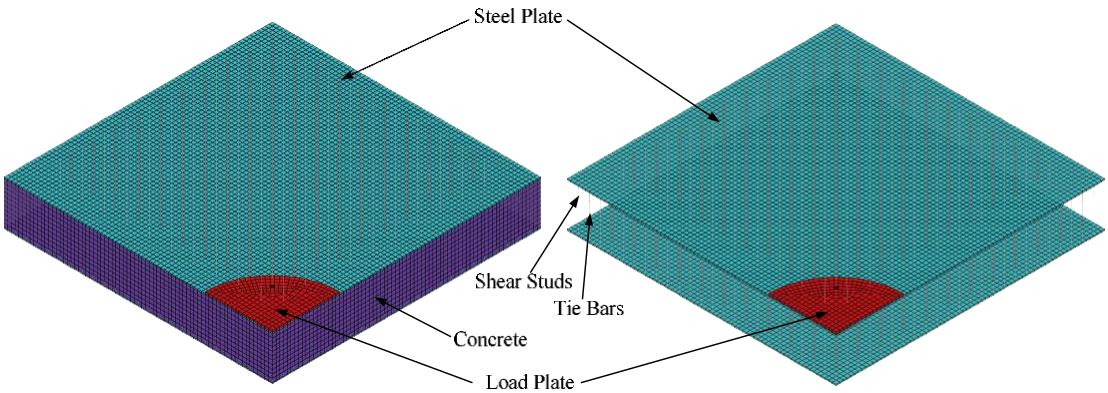

Figure 4. SC Wall FE Model.

Two support conditions, fixed and simply supported, were considered along the panel edges to facilitate the evaluation of membrane effects. Symmetry conditions were applied to the axi-symmetric boundaries. For the simply supported case, translation was only restricted in the z-direction (the direction of the load) simulating a roller and thereby removing membrane effects.

FE ANALYSIS RESULTS

The FE models were modified to investigate the influence of tie bar spacing and diameter, reinforcement ratio, span to depth ratio, and size of the load plate. Table 1 lists the models run and which parameters were varied in each.

The column labeled "$M_n/(V_nT)$" relates the moment to shear capacity. M_n and V_n are computed in accordance with the provisions of AISC N690, Appendix N9 (Draft). This ratio provides an indication of what type of behavior is critical when compared to the shear span to depth ratio (*S/T*). If *S/T* is greater than the value of $M_n/(V_nT)$ the behavior is flexural controlled. If *S/T* is less than $M_n/(V_nT)$, shear behavior is expected to dominate. Thus, for higher ratios of moment to shear capacity, it is more likely that shear behavior will dominate behavior. For lower values, it requires unusual load cases to force shear controlled behavior. The column labeled "M_n" provides the moment capacity per unit width of the panel.

The column labeled "P_n" provides the collapse load computed by yield line analysis ($P_n \sim 12.6M_n$ for loads distributed over a small footprint). This is the total collapse load; because the models are axi-symmetric, the maximum load in the model should be approximately one-quarter of value reported in the table. For the majority of the cases run for this study, the load at yield was approximately 75% of this theoretical collapse load.

To confirm realistic behavior, two models were run with gradually increasing uniform loads applied to the top surface nodes (F_T2_S/T24_U and S_T2_S/T24_U in Table 1). Yield line theory suggests a 79 psi collapse load for the fixed support case and 39.5 psi for the simple support case. Results from these models produced collapse loads close to the loads at which the panels began to yield. Model results also showed that the fixed support case demonstrated greater initial stiffness than the simple support case and gains strength from membrane action before failure.

Before discussing the influence of design parameters, it is important to understand the general behavior of an SC panel as the load increases. Representative behavior of fixed and simply-supported SC panels is shown in Figure 5. The lettered points in Figure 5 correspond to the following behavior:

A – concrete reaches tensile strength

B – concrete reaches compressive strength

C – bottom steel plate reaches yield strength (near perimeter of load surface)

D – first tie bar ruptures

E – bottom steel plate ruptures completely

As explained in more detail later in this paper in the section on biaxial considerations, because of the biaxial stress state of the steel plates, the uniaxial effective failure strain of 0.146 is unrealistic. The rupture strain of the plates will be lower. To account for this effect and constraint effects from welded joints in actual structures, a failure strain of 0.05, as recommended in NEI 07-13 (2009), is more realistic. The point E' on Figure 6 shows the point at which this failure strain would lead to rupture of the bottom steel plate. Point E' is recommended for design purposes rather than E.

Table 1. FE Cases.

Model Name*	Tie Bar Spac. (in)	Tie Bar & Shear Stud Dia. (in)	Steel Plate Thk. (in)	Total Thk. (in)	Reinf. Ratio (%)	Load Plate Size (ft)	$M_n/(V_nT)$ **	M_n (kip·ft/ft)	P_n (kip)
F_T/2_Stud0.75	15	0.75	0.75	30	5.0	7.5	4.9	1080	13500
F_T/2_Stud0.875	15	0.875	0.75	30	5.0	7.5	4.3	1080	13500
F_T/2_Stud1.0	15	1.0	0.75	30	5.0	7.5	3.7	1080	13500
F_T_Stud0.75	30	0.75	0.75	30	5.0	7.5	8.1	1080	13500
F_T/2_Stud0.75	15	0.75	0.75	30	5.0	7.5	4.9	1080	13500
F_T/4_Stud0.75	7.5	0.75	0.75	30	5.0	7.5	2.2	1080	13500
F_T/4_Stud0.875	7.5	0.875	0.75	30	5.0	7.5	1.8	1080	13500
S_T/4_Stud0.875	7.5	0.875	0.75	30	5.0	7.5	1.8	1080	6800
F_T/2_Rho5.0	15	0.75	0.75	30	5.0	7.5	4.9	1080	13500
F_T/2_Rho3.3	15	0.75	0.50	30	3.3	7.5	3.4	730	9200
F_T/2_Rho2.5	15	0.75	0.375	30	2.5	7.5	2.6	550	6900
F_T/2_S/T12	15	0.75	0.75	30	5.0	7.5	4.9	1080	13500
F_T/2_S/T18	10	0.75	0.50	20	5.0	7.5	3.3	480	6000
F_T/2_S/T24	7.5	0.75	0.375	15	5.0	7.5	2.2	270	3400
F_T/4_7.5ftCirc	7.5	0.875	0.75	30	5.0	7.5	1.8	1080	13500
F_T/4_2ftCirc	7.5	0.875	0.75	30	5.0	2.0	1.8	1080	13500
F_T/4_5ftCirc	7.5	0.875	0.75	30	5.0	5.0	1.8	1080	13500
F_T2_ S/T24_U	15	0.75	0.375	15	5.0	Uniform Load	8.7	270	10200 (79 psi)
S_T2_ S/T24_U	15	0.75	0.375	15	5.0	Uniform Load	8.7	270	5100 (39.5 psi)

*Nomenclature: F = fixed-support; S = simple-support; T = tie bar spacing; S/T = span-to-thickness ratio; Circ = circular load plate; Rho = reinforcement ratio; U = uniform pressure, Stud = tie bar and shear stud diameter.

** $M_n/(V_n T)$ has thickness, T, in denominator to make dimensionless

The sequential contour plots shown in Figure 6 further demonstrate the behaviors described above. The accumulated damage within the concrete core is shown fringed in the figure. Displayed is the greatest of brittle and ductile damage from tensile and compressive stresses, respectively.

Figures 7(a) through 7(e) summarize the effects of parameter variation on the load-displacement behavior of SC walls. The influence of each parameter is described in the following paragraphs. Note that all curves in Figure 7 are consistent with the theoretical representation in Figure 1, which constructs the resistance function, and consists of the initial linear elastic section of the curve and the linear displacement hardening section of the curve.

The size of the load plate influences the result - smaller load plates lead to highly localized failure. This is undesirable for this study of global response. As the load plate increases in size behavior changes: the yield load increases, ductility increases, and the panel reaches higher strength capacity. Initial stiffness is similar for all cases. As the purpose of this investigation is to evaluate global response, the response mode of interest is the progressive collapse of the plate following formation of a collapse mechanism. This type of failure occurs due to the accumulation of plate membrane strain produced, primarily, by plastic hinging of the composite section. To ensure it is this behavior and not localized failure in the remaining models, the

loading is applied over a circular footprint with a 7.5-ft diameter (approximately one-quarter of the panel span).

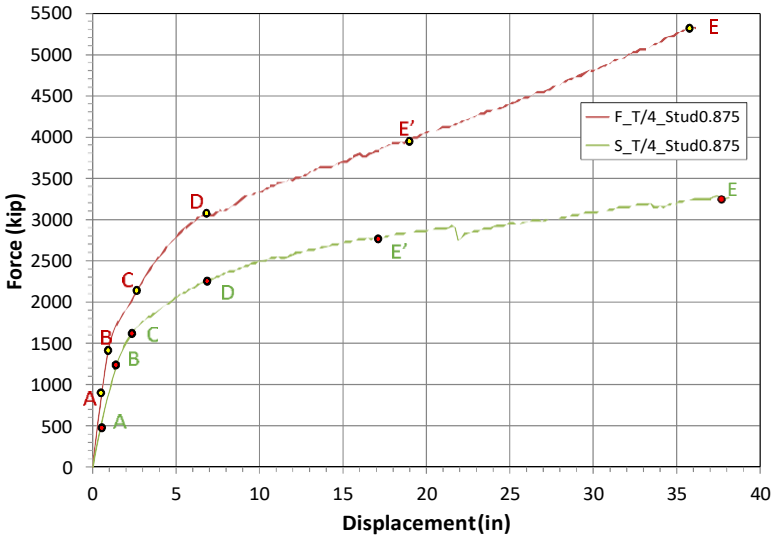

Figure 5. Typical SC Wall Load-Deformation Plot.

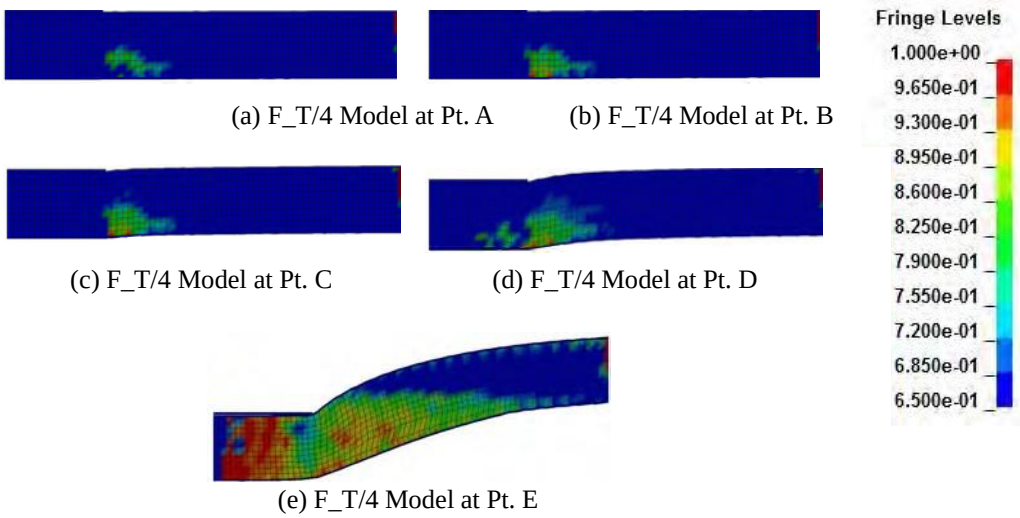

(a) F_T/4 Model at Pt. A (b) F_T/4 Model at Pt. B

(c) F_T/4 Model at Pt. C (d) F_T/4 Model at Pt. D

(e) F_T/4 Model at Pt. E

Figure 6. Sequential Concrete Damage Contour Plots for Typical SC Wall

The influence of the reinforcement ratio is as expected – lower reinforcement ratios lead to less capacity. For the steel plate reinforcement ratios considered in this study, the results showed that reinforcement ratio has negligible effect on available ductility. Because the behavior of these panels under point loads is dominated by concrete shear failure, the "yield" point is independent of the reinforcement ratio: ultimate strength depends on reinforcement ratio. Each of the peak strengths is similar to that expected from yield line analysis.

The influence of tie bar spacing is noticeable. More densely spaced bars slow shear crack growth and thereby increase the yield strength of the panel. They also lead to higher overall strength (approximately 20% increase in strength with tie bars spaced at T/4 when compared to T/2). The opposite effect is observed when tie bars are spaced further apart. Current SC design recommendations (AISC N690, Appendix N9, Draft) suggest spacing no further apart than T/2.

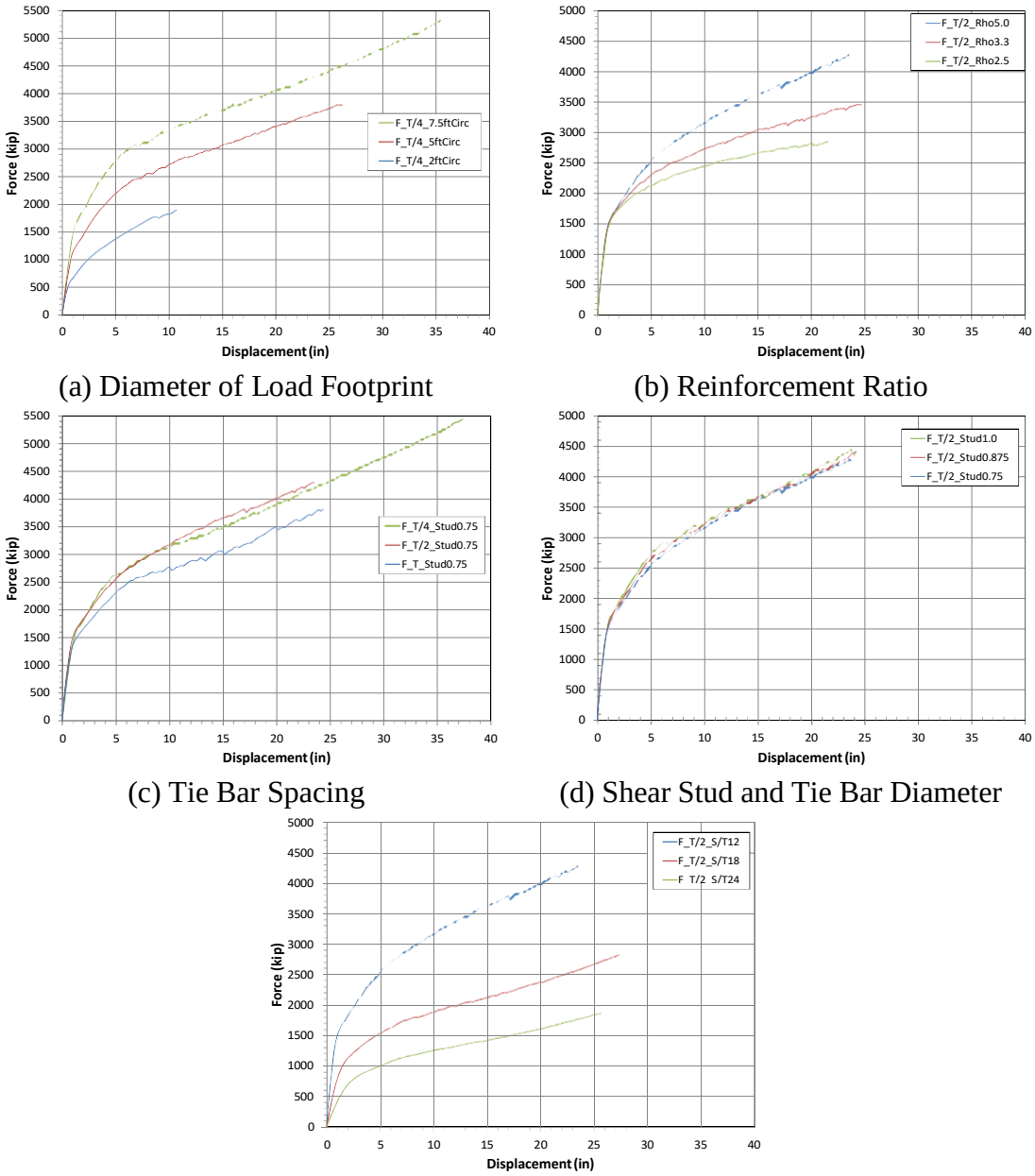

(a) Diameter of Load Footprint

(b) Reinforcement Ratio

(c) Tie Bar Spacing

(d) Shear Stud and Tie Bar Diameter

(e) Span to Thickness Ratio

Figure 7. Effect of System Parameters on Resistance Function.

The influence of tie bar diameter is negligible. The panel with 0.75-in diameter bars spaced at T/2 was designed in accordance with recommendations of

AISC N690, Appendix N9 (Draft). For a given tie bar spacing, increasing the tie bars size slightly does not increase the strength by a large margin nor does it prevent the shear dominated behavior from occurring. Tie bar spacing has more influence on shear strength than tie bar size has on shear strength.

The influence of span to depth ratio is similar to RC panels. As S/T decreases so does the ductility. For S/T of 24, observed ductility is about 65% of that for an S/T of 12.

BIAXIALITY CONSIDERATIONS

The governing failure response mechanism for an SC wall panel subjected to impulsive loading has been demonstrated to be characterized by ductile tensile rupture of the bottom plate resulting from large biaxial membrane strains. Ductile tensile rupture occurs at a lower effective strain for a plate loaded in biaxial membrane tension than for the uniaxial condition. This reduction in effective strain, $\varepsilon = \sqrt{\varepsilon_{\frac{1}{2}} + \varepsilon_{\frac{1}{2}}}$, at rupture, which has been investigated by others (Nickell et al., 2003; Manjoine, 1983), is a function of the material strain hardening exponent and a triaxiality factor, T, defined by

$$T = \frac{\sqrt{2}(\sigma_1 + \sigma_2 + \sigma_3)}{\sqrt{(\sigma_1 - \sigma_2)^2 + (\sigma_2 - \sigma_3)^2 + (\sigma_3 - \sigma_1)^2}} \tag{3}$$

For a centrally loaded square plate with fixed or simply supported edges, with near symmetrical biaxial stresses and strains in the vicinity of the loading, $T \sim 2.0$. The ratio of biaxial failure strain, ε_f, to uniaxial failure strain, ε_t, is a function of material strain hardening exponent, n ($n \sim 0.21$ for mild steel), and the triaxiality factor, $T = 2$. After Nickell et al. (2003),

$$\frac{\varepsilon_f}{\varepsilon_t} = \frac{\sinh\left[\frac{\sqrt{3}}{3}(1-n)\right]}{\sinh\left[\frac{\sqrt{3}}{3}(1-n)T\right]} = 0.46 \tag{4}$$

Note that for T in the range of 2, $\varepsilon_f / \varepsilon_t$ is relatively insensitive to n (for $0 < n < 1$). Manjoine (1983) proposed a failure strain limit, based on empirical studies, as

$$\frac{\varepsilon_f}{\varepsilon_t} = 2^{(1-T)} = 0.50 \tag{5}$$

The two values are in close agreement and the higher one is selected. Applying a factor, α, as a margin on structural capacity for plastic tensile instability under a uniform biaxial membrane strain state resulting from impulsive loading, and considering 0.146 as the effective uniaxial failure strain, the allowable effective

failure strain is α x 0.5 x 0.146. Selecting α = 0.7, the allowable effective failure strain would be 0.05. The displacement on the resistance function curve corresponding to this effective strain limit, $\varepsilon = \sqrt{\varepsilon_X^2 + \varepsilon_Y^2}$, then represents the design allowable plate central displacement limit for assessment of the response determined by solution of Eq. (2).

CONCLUSIONS AND RECOMMENDATIONS

The load-deformation behavior of impulsively loaded SC panels has been investigated using pseudo-static nonlinear finite element studies. These solutions demonstrate, for a properly designed panel, a structural response sequence defined by localized failure of the concrete, yielding of the bottom plate, tie bar rupture and load displacement strain hardening of the system until the bottom steel plate ruptures. The resistance function exhibits a near-linear displacement hardening effect over the entire plastic range, until rupture. Due to tension stresses which develop in the plates to resist shear, and the increase in shear force resultant with decreasing interface footprint dimension, the load deformation curve is dependent on footprint size.

Based on biaxiality considerations, an allowable central displacement in the steel plate corresponding to development of an allowable effective biaxial strain can be calculated. While the allowable ductility for SC walls may be less than that of RC walls, the much larger reinforcement percentage for SC walls affords them superior impact resistance.

A design-by-analysis approach, consisting of development of the panel resistance function, representation of the impulsively loaded panel as an equivalent SDOF system, and solution of the nonlinear equilibrium equation for the panel response has been presented.

It is recommended that pseudo-static and dynamic testing be performed to further confirm and assess the behaviors identified in this investigation.

REFERENCES

AISC N690. (Draft). “Specification for Safety-Related Steel Structures for Nuclear Facilities Supplement No. 1.” Appendix N9, American Institute of Steel Construction.

Anderson, N., and Meinheit, D. (2000). “Design Criteria for Headed Stud Groups in Shear: Part 1 - Steel Capacity and Back Edge effects.” *PCI Journal*, 45(5), pp. 46-75.

ASCE Manual of Practice No. 58. (1980). *Structural Analysis and Design of Nuclear Plant Facilities*, American Society of Civil Engineers, New York, NY.

Biggs, J. (1964). *Introduction to Structural Dynamics*, McGraw-Hill, Inc.

Bruhl, J. C., Varma, A. H., and Johnson, W. H. (2013). “Design of SC Composite Walls for Projectile Impact: Local Failure.” *Transactions of the 22nd SMiRT*. San Francisco, CA.

LSTC. (2012). *LS-DYNA Keyword User’s Manual: Volume II Material Models*, (V971 R6.1.0 ed.), Livermore Technology Software Corporation, Livermore, CA.

Manjoine, M. J. (1983). "Damage and Failure at Elevated Temperature." *Transactions of the ASME Journal of Pressure Vessel Technology*, pp. 58-62.

Mizuno, J., Koshika, N., Tanaka, E., Suzuki, A., Mihara, Y., Nishimura, I. (2005). "Investigation on Impact Resistance of Steel Plate Reinforced Concrete Barriers Against Aircraft Impact Part 3: Analyses of Full-Scale Aircraft Impact." *Transactions of the 18th SMiRT*, pp. 2591–2603, Beijing, China.

Murray, Y. D. (2007). "Users Manual for LS-DYNA Concrete Material Model 159." Report No. FHWA-HRT-05-062, Federal Highway Administration.

NEI 07-13. (2009). "Methodology for Performing Aircraft Impact Assessments for New Plant Designs." Nuclear Energy Institute.

Nickell, R. E., Duffey, T. A. and Rodriguez, E. A. (2003) "ASME Code Ductile Failure Criteria for Impulsively Loaded Pressure Vessels." *2003 ASME Pressure Vessels and Piping Conference*.

Shim, C.-S., Lee, P.-G., and Yoon, T.-Y. (2004). "Static Behavior of Large Stud Shear Connectors." *Engineering Structures*, 26(12), pp. 1853–1860.

Tsubota, H., Kasai, Y., Koshika, N., Morikawa, H., Uchida, T., Ohno, T., Kogure, K. (1993). "Quantitative Studies on Impact Resistance of Reinforced Concrete Panels with Steel Liners Under Impact Loading Part 1: Scaled Model Impact Tests." *Transactions of the 12th SMiRT*, pp. 169–174, Stuttgart, Germany.

UFC 3-340-02. (2008). "Structures to Resist the Effects of Accidental Explosions." U.S. Department of Defense, Washington, D.C.

Varma, A. H. (2000). *Seismic Behavior, Analysis, and Design of High Strength Square Concrete Filled Steel Tube (CFT) Columns*. Lehigh University.

Zhang, K., Varma, A. H., and Gallocher, S. (2013). "Partial Composite Action in SC Composite Walls for Nuclear Structures." *Transactions of the 22nd SMiRT*, San Francisco, CA.